Heavy minerals and garnet geochemistry of stream sediments and bedrocks from the Almklovdalen area, Western Gneiss Region, SW Norway: implications for provenance analysis

Anne Krippner [1,*], Guido Meinhold [1], Andrew C. Morton [2,3], Jan Schönig [1], Hilmar von Eynatten [1]

[1]Department of Sedimentology and Environmental Geology, University of Göttingen, Goldschmidtstraße 3, 37077 Göttingen, Germany

[2]CASP, West Building, 181A Huntingdon Road, Cambridge CB3 0DH, United Kingdom

[3]HM Research Associates, 2 Clive Road, Balsall Common, West Midlands CV7 7DW, United Kingdom

* Corresponding author:
Tel.: +49 551 3910297, fax number: +49 551 397996
E-mail address: Anne.Krippner@geo.uni-goettingen.de (A. Krippner)

Keywords: heavy minerals; garnet geochemistry; compositional biplot; provenance; Almklovdalen peridotite massif

Abstract

Detrital heavy minerals commonly document the geological setting in the source area, hence they are widely used in sedimentary provenance analysis. In heavy mineral studies most commonly the 63−125 and 63−250 µm grain-size fractions are used. Heavy mineral data and garnet geochemistry of stream sediments and bedrocks from the catchment area draining the Almklovdalen peridotite massif in SW Norway reveal that a wider grain-size spectrum needs to be considered to avoid misleading interpretations. The Almklovdalen peridotite massif consists mainly of dunite and harzburgite, as testified by the heavy mineral suite. At the outlet of the main river the heavy mineral spectrum is very monotonous due to dilution by strong influx of olivine. Heavy minerals like apatite and epidote characterising the host gneisses have almost disappeared. MgO-rich almandine garnets are more frequent in the coarser grain-size fractions, whereas MnO-rich almandine garnets are more frequent in the finer grain-size fractions. Garnets with pyrope content exceeding 50 % are only found in the 500−1000 µm grain-size fraction. Therefore, the sample location and the selected grain-size fraction

are of paramount importance when dealing with heavy minerals and mineral geochemical data, otherwise, provenance sensitive information may be missed.

1. Introduction

Heavy minerals are used to characterise, discriminate, and identify source areas (Mange and Wright, 2007; von Eynatten and Dunkl, 2012, and references therein). Commonly the heavy mineral composition of a sediment reflects the mineralogy of the rocks exposed in the source area, however, the heavy mineral assemblage may be affected by several processes during the sedimentary cycle that modify occurrence and proportions of heavy mineral species (e.g., Morton and Hallsworth, 1999). For instance, the stability of heavy minerals strongly depends on the specific environment and climatic conditions (Pettijohn, 1941; Morton and Hallsworth, 1999; Velbel, 2007; Andò et al., 2012; Morton, 2012; Garzanti et al., 2013). Therefore, differences in heavy mineral ratios are not necessarily the effect of different sources, but can reflect modifications which occur during the sedimentary cycle (e.g., Morton and Hallsworth, 1999). When studying stream sediments it must be noted that minerals can be segregated and sorted according to their grain size, density, and shape (Morton and Hallsworth, 1999; Garzanti et al., 2008, 2009; Resentini et al., 2013). This can happen either between different heavy mineral species, but also within a single mineral group. For example, almandine-rich garnets are commonly concentrated in the finer fractions in contrast to less dense garnet species (Schuiling et al., 1985; Andò, 2007; Garzanti et al., 2008).

The heavy mineral garnet has important provenance applications, because it exists in a wide range of rocks and its chemical composition depends on the composition of the source rock and on pressure and temperature conditions during garnet formation (e.g., Wright, 1938; Morton, 1985; Deer et al., 1992; Andò et al., 2013; Krippner et al., 2014). Although garnets from various garnet-bearing rocks often show much overlap in major element geochemistry, mantle-derived garnets, for instance, can be very well separated from crustal-derived garnets (e.g., Krippner et al., 2014). Therefore, garnet is used as an indicator mineral in exploration, for instance, for diamond (Nowicki et al., 2003) because mantle-derived garnets can be related to diamond-bearing intrusives (Grütter et al., 2004). In contrast to the typical mantle-derived minerals olivine and pyroxene, garnet is more stable during alteration and

dispersion at the Earth's surface (e.g., Pettijohn, 1941; Velbel, 1984, 1999; Gurney, 1984; Grütter et al., 2004; Morton, 2012).

We collected stream sediments and adjacent source rocks in the high-grade metamorphic Almklovdalen area in SW Norway to study to what extent the heavy mineral suites and garnet composition of the stream sediments reflect the mineralogy of the source rocks. We analysed different grain-size fractions in order to test for grain-size dependency of heavy mineral assemblages and garnet geochemistry which may lead to ambiguous or even wrong interpretations when a single and narrow grain-size spectrum is considered only (Garzanti et al., 2009).

2. Geological Setting

The Almklovdalen area is located in the Western Gneiss Region (WGR) in SW Norway (Fig. 1). The WGR comprises Precambrian basement and allochthonous cover units, metamorphosed and deformed during the Caledonian orogeny induced through collisions between Baltica, Laurentia and Avalonia under closure of Iapetus Ocean (Roberts and Gee, 1985; Cuthbert et al., 2000; Krabbendam et al., 2000; Beyer et al., 2012). The gneisses and augen orthogneisses of the WGR are mainly of granodioritic to granitic composition and are considered to represent Baltica basement (Tucker et al., 1990). The gneisses are predominantly of amphibolite-facies metamorphic grade (Bryhni and Andréasson, 1985; Krabbendam and Wain, 1997; Krabbendam et al., 2000), but in some parts granulite-facies assemblages occur (Griffin et al., 1985; Krabbendam et al., 2000). Most of the orthogneisses of the WGR are suggested to be generated during Gothian (1.7−1.5 Ga) and Sveconorwegian (1.2−1.9 Ga) events (Beyer et al., 2012). During the Scandian phase (435−390 Ma) of the Caledonian orogeny, rocks of the WGR suffered high-pressure (HP) to ultrahigh-pressure (UHP) conditions (Griffin and Brueckner, 1980, Gebauer et al., 1985; Griffin et al., 1985; Mørk and Mearns, 1986; Andersen et al., 1991; Krabbendam et al., 2000). The metamorphic grade increases from SE to NW (Krogh, 1977; Cuthbert et al., 2000; Root et al., 2005; Beyer et al., 2012). The temperature gradient increases from ~550 °C in the SE to >800 °C in the NW (Krogh, 1977; Griffin et al., 1985; Carswell and Cuthbert, 2003). Mafic and ultramafic lenses which are enclosed within the surrounding gneisses range in size from centimetres to hundreds of metres (Carswell and Cuthbert,

2003). A few ultramafic bodies reach sizes up to several kilometres. There are hundreds of mantle-derived ultramafic bodies (Beyer et al., 2012), with some of them containing garnet-bearing assemblages (Eskola, 1921; Medaris, 1984; Carswell, 1986; Medaris and Carswell, 1990; Brueckner et al., 2010; Beyer et al., 2012). The ultramafic rocks show Archaean Re−Os ages which predate the formation of the Proterozoic upper crusts in the region (Brueckner et al., 2002; Beyer et al., 2004). One of the largest ultramafic body, with a size of 4.0 × 3.3 km^2, is the Almklovdalen peridotite (Medaris and Brueckner, 2003), located in the HP−UHP transition zone (Fig. 1). This ultramafic body is a bowl-shaped sheet around a central gneiss area, composed of orthogneisses and paragneisses and indicates three main stages of deformation. A first deformation is seen in the Proterozoic folds in the garnet peridotite, a second deformation is highlighted by the Caledonian isoclinal folds in the chlorite peridotite in association with recrystallisation of garnet peridotite to chlorite peridotite, and a third deformation – also Caledonian in age – led to foliations and lineations in chlorite peridotite (Medaris and Brueckner, 2003). The main rock types in the Almklovdalen body are anhydrous dunite and harzburgite (Osland, 1997; Medaris and Brueckner, 2003; Beyer et al., 2006, 2012). They contain garnet peridotite and garnet pyroxenite lenses (Medaris, 1984; Osland, 1977; Beyer et al., 2012), which occur in <40 cm thick bands within the dunites and harzburgites (Cordellier et al., 1981). Eclogites are also present, but only in minor amounts (Griffin and Qvale, 1985; Beyer et al., 2012). The Almklovdalen body is surrounded by orthogneisses, paragneisses, anorthosites, and eclogites (Beyer et al., 2012).

3. Samples and methods

3.1 Samples

Four sand samples were collected from streams draining the Almklovdalen peridotite body (Fig. 2). Loose bedload sand was sampled to cover a wide grain-size range. Stream sample AK-N20 was collected ~1 km SE of Helgehornet, followed by sample AK-N19-4 further downstream (Fig. 2). Stream sample AK-N19-3 was taken from the middle part of the Gusdalselva river and stream sample AK-N19-1 comes from the mouth of the Gusdalselva river entering lake Gusdalsvatnet. In addition, bedrock samples were collected since they represent the source for the detrital material. Bedrock

samples were taken in outcrop. One bedrock sample, a large pebble, was taken directly from the river bed. Sample AK-N21 is an eclogite exposed south of Helgehornet and AK-EA is an eclogite pebble collected at the mouth of the Gusdalselva river. Sample AK-N24 is a garnet peridotite and AK-N25 is a gneiss exposed SE of Helgehornet. The geographic coordinates of all samples are given in Table 1.

3.2 Methods

Stream sediments were wet-sieved using a mechanical shaker to separate the different grain-size fractions (63−125 μm, 125−250 μm, 250−500 μm, 500−1000 μm). We used ~ 350 grams per sample. After drying, the samples were treated with acetic acid to remove the carbonate component if present. The heavy mineral fractions were separated using Sodium polytungstate (SPT) with a density of 2.85 g/mL.

The heavy mineral residues were mounted on microscope slides (Mange and Maurer, 1992) using Meltmount™ with refraction of 1.66 and identified under the polarising microscope. The relative abundances of the heavy minerals were determined by grain counting. For that, the microscope slide was moved along linear traverses and all grains between two parallel lines were counted (i.e. ribbon counting; Mange and Maurer, 1992). Two-hundred and fifty translucent minerals were counted for each slide. All data are given as supplementary data, i.e. data of all heavy minerals including opaque minerals, micas and unknown (Supplementary Table S1), only groups of transparent minerals (see Supplementary Table S2), and heavy minerals from all grain-size fractions (Supplementary Table S3). Unknown mineral are probably originated by alteration of various minerals and are aggregates with no well defined mineralogical composition. They are also termed as alterites (van Andel, 1950).

For garnet geochemical analysis, garnet selection from the stream sediments was achieved by handpicking under a binocular microscope. We randomly selected garnet grains of all sizes and morphological types and placed them in synthetic mounts using a bonding epoxy composed of a mixture of Araldite® resin and hardener in the ratio of 5:1. Grains of different morphological types were selected to consider a wide range of altered and non-altered garnets in the source area. Also garnets of different colours in approximately similar amounts were selected to minimize the bias of picking only one type of garnet.

From the bedrock samples polished thin sections were prepared. Garnet from bedrock and stream samples were analysed with a JEOL JXA 8900 RL electron microprobe (EMP) equipped with five wavelength dispersive spectrometers at the University of Göttingen (Department of Geochemistry, Geoscience Center). Before analysis, all samples were coated with carbon to ensure conductivity. Conditions included an accelerating voltage of 15 kV and a beam current of 20 nA. The counting times were 15 seconds for Si, Mg, Ca, Fe, and Al, and 30 seconds for Ti, Cr, and Mn (Table 2). Matrix correction was performed using ZAF corrections. We preferentially analysed garnet rims and cores. From the thin sections 20 garnets from each sample were analysed and 50 garnets of each sediment sample were measured. Additionally, minerals in thin sections were determined under the polarising microscope. The relative abundances of the main light and heavy minerals from the bedrocks can be taken from Table 3. The full database including lithology and metamorphic grade are included in Supplementary Table S4.

From all stream sediment samples the 63−125 µm fractions were point counted and analysed by EMP. For the study of grain-size dependency sample AK-N19-3 was chosen. From this sample the 125−250 µm and 250−500 µm grain-size fractions were point counted, too, and garnet grains from the 125−250 µm, 250−500 µm and 500−1000 µm size fractions were analysed by EMP.

We measured the long and short axes of ~100 garnet grains from the 63−125 µm grain-size fraction of each river sample, to study if the garnets are mainly separated by their short axis or mainly by their long axis and if there is an appreciable input of garnets with smaller or coarser grain size, which are not belonging to the specific grain size fraction. Long and short axes of garnet from bedrocks (AK-N21, AK-EA, AK-N24) were also measured for comparison (Supplementary Table S5).

The geochemical data are presented in ternary diagrams following Mange and Morton (2007) and in biplots produced using CoDaPack, an open source software for compositional data analysis (Thió-Henestrosa and Martín-Fernández, 2005; Comas-Cufi and Thió-Henestrosa, 2011). The biplots are based on principal component analysis (PCA) using centred log-ratio transformation for six major element oxides, following the methodology proposed by Aitchison (1986). The biplots serve as a valuable tool for estimating the potential for discrimination of a multivariate data set and its subsets (e.g., von Eynatten et al., 2003). In biplots, multivariate observations are illustrated as points and

variables as lines. The length of the line corresponds to the variability of the respective element. Length and position of the line reflects its relative influence on the respective principal component.

4. Results

4.1. Heavy mineral analysis of all stream samples (63−125 µm)

In all stream samples, olivine is the dominant heavy mineral representing between 39 and 90 % of the heavy mineral suite (Fig. 3a). Pyroxene comprises between 8 and 11 % (mainly diopsitic to augitic clinopyroxenes). Garnet, green calcic amphibole, epidote-group minerals (epidote, zoisite), and apatite occur in different percentages. The amphiboles are dominantly blue-green with colour changing from blue-green to green. Ultrastable minerals (zircon, tourmaline, and rutile) are not present or occur only in traces. Other amphiboles (mainly actinolites and tremolites) and titanites occur occasionally as single grains in individual samples and are grouped as 'others'. Opaque minerals and micas are not considered in the diagram to emphasize the relative concentrations of the transparent heavy minerals.

4.2. Heavy mineral analysis of sample AK-N19-3 (63–125 µm, 125–250 µm, 250–500 µm)

Olivine is the dominant heavy mineral with similar amount (59–63 %) in all grain-size fractions (Fig. 3b). Garnet content is higher in the coarser grain-size fractions, i.e. 28 % in the 125–250 µm fraction and to 24 % in the 250–500 µm fraction compared to 9 % in the 63–125 µm fraction. In contrast, pyroxene and green calcic amphibole decrease in the coarser fractions. The content of epidote-group minerals remains fairly constant, whereas apatite (5 %) is only found in the 63–125 µm grain-size fraction. Ultrastable minerals are almost absent in the 250–500 µm fraction. The 500–1000 µm grain-size fraction is not considered here because of the very high proportion of micas and opaque minerals, which amounts to almost 90 % of the entire heavy mineral spectrum.

4.3. Grain-sizes of garnets

The shortest axes of garnets from the 63–125 µm sieve fractions of the stream sediments range from >40–180 µm and the longest axes range from >80–300 µm (Fig. 4; Supplementary Table S5). The

shortest axes of garnets from the eclogite bedrocks are between <100–700 μm and the longest axes between 100 μm to >1000 μm (Fig. 4; Supplementary Table 5).

The garnets of sample AK-N24 (garnet peridotite) are very coarse and go beyond the camera's field of view of the microscope. The shortest axis of the smallest grain found in this sample is 1000 μm and the longest axis of the largest grain is about 1.4 cm (measured with a ruler).

4.4. Geochemistry of garnets

Biplots with the major element oxides SiO_2, Al_2O_3, CaO, MgO, FeO, and MnO as variables are used to differentiate garnets from the different bedrock types and from the sediments (Fig. 5). These diagrams are optimal in the sense that most of the total variability is illustrated in two dimensions (i.e. 89–99% in this case). SiO_2 and Al_2O_3 show the lowest variation in all of the three biplots (Figs. 5a, 5b, 5c). The small distance between SiO_2 and Al_2O_3 indicates relatively constant SiO_2/Al_2O_3 ratios typical for all garnet varieties with aluminum in the crystallographic Y-site (i.e. endmembers almandine, spessartine, pyrope, grossular).

The major element data of the garnets from the bedrocks show highest variability for MnO and MgO (spread in opposite directions and strongly controlling PC1) and a moderate variability for CaO and FeO along with fairly constant CaO/FeO (Fig. 5a). The three bedrock samples are clearly separated from each other in the biplot, with garnets from the peridotite being distinct due to relative high MgO content. Garnets of the eclogites accumulate on the left side of the biplot indicating relatively lower MgO content, with garnets of sample AK-N21 appearing to have slightly higher relative MnO content (i.e. higher MnO/CaO ratios), when compared to eclogite sample AK-EA (Fig. 5a).

The detrital garnets show a comparably high variability for MnO, MgO and CaO (spread in different directions) and show much overlap between both different samples and different grain-size fractions (Fig. 5b, 5c). The CaO/FeO value is no longer constant, particularly for the coarser grain-size fraction (Fig. 5c). CaO and MnO have the highest impact on PC2, which in turn has much higher impact on the total variability of the detrital garnets (22 and 26%) compared to the bedrocks (7%; Fig. 5). This implies higher relevance of CaO/MnO ratios for the variability of the detrital garnets. The detrital garnets of the different grain-size fractions of sample AK-N19-3 show only little contrast. However,

few garnets of the coarser grain-size fractions (250−1000 μm) show overlap with the garnet peridotite (Fig. 5c).

Garnet composition from stream sediments and bedrocks is illustrated in the classical ternary classification diagram using almandine + spessartine, pyrope, and grossular as poles, and the discrimination fields A, B, Bi, Ci, Cii, and D (Mange and Morton, 2007; Fig. 6). This diagram has widely been applied in a number of garnet provenance studies (e.g., Whitham et al., 2004; Morton et al., 2005; Mange and Morton, 2007; Meinhold et al., 2010; Morton et al., 2011; Krippner et al., 2015). All of the garnets of samples AK-EA and almost all of the garnets of sample AK-N21 plot in field Ci, the field for garnets derived from high-grade mafic rocks, such as eclogites. Garnets of sample AK-N24 plot in field Cii, the field for garnets derived from ultramafic rocks (Fig. 6a).

For comparison, all garnets from the stream sediments (63−125 μm grain-size fraction) and from the bedrocks are plotted together in one ternary diagram (Fig. 6b). The garnets from the stream sediments overlap fields B, Ci, A, and Cii, with almost 90 % of garnets plotting in field Ci. They show a high degree of overlap with garnets measured in the eclogites. However, many detrital garnets are not comparable to the garnets derived from the eclogites as they show a wider distribution and are possibly derived from other source rocks than the measured eclogites. Interestingly, no detrital garnets are comparable with those garnets measured in the garnet peridotite (Fig. 6b).

The garnets from the different grain-size fractions from sample AK-N19-3 overlap fields B, Bi, A, Ci, Cii, with almost 90 % plotting in field Ci. Many garnets show a high degree of overlap with garnets measured in the eclogites, but many garnets tend to higher MgO composition and also towards higher CaO or FeO+MnO composition. Two single garnets of the 500−1000 μm grain-size fractions show overlap with the garnets measured in the peridotite (Fig. 6c). Overall, the detrital garnets show a distinct higher variability than the garnets from the bedrocks, hence point to even other source rocks than the measured ones.

With increasing grain size the MgO/MnO value increases on average (Fig. 7). About 6% of the garnets of the coarser grain-size fractions (250−1000 μm) lie above line 2 comparing to 1% of the finer grain-size fraction (125−250 μm). None of the garnets of the 63−125 μm grain-size fraction lie above line 2.

In contrast, 18% of the garnets of the finer grain-size fractions (63−250 μm) and only 4% of the coarser grain-size fractions (250−1000 μm) lie below line 1. This is because the content of MnO is overall higher in the finer grain-size fractions (63−250 μm) than in the coarser grain-size fractions. In contrast, the MgO content of the coarser grain-size fractions (250−1000 μm) is higher on average compared to the finer grain-size fractions (Fig. 7). MnO contents exceeding 2 wt.% are only evident in the garnets of the finer grain-size fractions (63−250 μm) (Supplementary Table S4).

5. Discussion

Heavy mineral analysis of stream samples from the Almklovdalen area in SW Norway reveal an increase of olivine from upstream (AK-N19-4) to downstream (AK-N19-1) from ~40 to 90 % (Fig. 3a) and a decrease of green calcic amphibole from ~13 to ~1 %. The content of ultrastable minerals decreases, too. The content of garnet slightly increases in the middle part of the river and decreases at the downstream end of the Gusdalselva river where only 1 % garnet is found (sample AK-N19-1). Apatite grains decrease strongly from upstream to downstream. In sample AK-N19-4, approximately 11 % of the heavy mineral assemblage consists of apatite minerals, in sample AK-N19-1, at the downstream end of the Gusdalselva river, apatite grains were not found. Epidote-group minerals commonly occur in the upper section of the river (~10 %) but at the downstream end of the Gusdalselva river they are strongly depleted (~1 %). The pyroxene content is nearly constant in all samples (around 10%). Most of the pyroxenes are clinopyroxenes, probably of diopsitic to augitic composition and likely derived from the lherzolites (Beyer et al., 2006). However, there are also some orthopyroxenes identified which are probably of enstatitic composition.

Chlorite peridotite (dunite, harzburgite) covers a large area in the downstream part of the Gusdalselva river, including a huge quarry (Fig. 2), thus explaining the downstream increase in olivine concentration. In the upper part of the river, garnet peridotites, eclogites and gneisses are more frequent than in the downstream part of the river. Therefore, in samples AK-N19-3, AK-N19-4, and AK-N20 the influx from those rocks is higher than in sample AK-N19-1. Further downstream most of the heavy minerals are diluted by the high input of olivine. Apatite is found in the gneisses (Table 3). There is a major input of apatite recorded in sample AK-N19-4, which is not surprising since this part

of the river is draining the gneisses upstream from the sample location. The strong decrease of apatite minerals is likely due to the dilution process described before but may also result from partial dissolution, because apatite becomes unstable under acidic conditions (Morton, 2012). The vegetation of the study area and its surroundings consist mainly of coniferous forest and indicates a rather acidic environment in which apatite is prone to dilution.

The main lithologies in the study area are dunite and harzburgite with minor garnet peridotite, eclogite, and gneiss. The major garnet-bearing rocks are garnet peridotites and eclogites. In the sampled gneiss no garnet grains were found, but garnet-bearing gneisses are known from the surrounding area; hence, they also provide a source for the detrital garnets in the stream sediments. The detrital garnets of the 63−125 μm grain-size fraction show a high degree of overlap with the garnets analysed in the eclogites (Fig. 6b). However, many of the detrital garnets cannot be directly linked to the studied eclogites. A possible explanation is that the several eclogite bodies exposed in the area cover a range of different garnet compositions, which is also evident from the two measured eclogites as seen in the biplots, because they can be clearly separated from each other (Fig. 5a). This separation is only possible when FeO and MnO, respectively almandine and spessartine, are not combined. That is why a discrimination of both eclogites cannot be determined in the ternary diagrams. Garnets with a high MnO and a low MgO content can be probably linked to the garnet-bearing gneisses, which suffered lower grade amphibolite-facies metamorphism (Bryhni and Andréasson, 1985; Krabbendam and Wain, 1997; Krabbendam et al., 2000). There is no overlap of detrital garnets with the garnets from the garnet peridotite. This suggests that the eclogites and the gneisses are the main source of the detrital garnets. Due to the fact that the grain size of the garnets in the garnet peridotite is coarser (the short axis of the smallest grain is >1000 μm) than the garnets in the studied 63−125 μm grain-size fraction, it is not very likely that these garnets occur in this grain-size fraction. Of course, coarse-grained source rock garnets, crushed through hydraulic or other mechanical processes, can occur in the finer grain-size fractions, but less likely than garnets with an original finer size distribution in the source rocks. In contrast, garnets of original finer size distribution in the source rocks cannot be expected in the coarse grain-size fractions. Therefore, it can be assumed that lower grade metamorphic garnets, possibly derived from the garnet-bearing gneisses, are generally finer,

because almandine garnets with higher MnO content are more frequent in the finer grain-size fractions (Fig. 7). In the ternary diagram, only two detrital garnets of the very coarse 500−1000 µm grain-size fraction overlap with the garnets from the peridotites (Fig. 6c). In the biplots (Fig. 5c), this number is slightly higher and includes grains from the 250−500 µm, too. Therefore, a general coarse grain size of garnets from the garnet peridotites exposed in this area can be assumed, as observed in the bedrock sample AK-N24, too. The fact that only grains from the coarse grain-size fractions show overlap with the garnet peridotite (Figs. 5c, 6c) is likely due to the inheritance of grain size from source rock to sediment. Alternatively, the peridotites contribute only little detritus to the sediment and the number of 50 garnets measured from the 63−125 µm grain-size fraction is insufficient to detect them. As an effect of hydraulic sorting during settling, heavy minerals concentrate in specific grain-size classes (Rubey, 1933; Rittenhouse, 1943; Garzanti et al., 2008; Resentini et al., 2013). The specific endmembers of garnet show different densities, with the highest density of ~ 4.3 g/cm³ for almandine garnets, 4.2 g/cm³ for spessartine garnets and 3.6 g/cm³ for pyrope garnets (Deer et al., 1992). Commonly, garnets with a higher density are found in the fine tail of the grain-size distribution in contrast to less dense garnet species (Schuiling et al., 1985; Andò, 2007; Garzanti et al., 2008). Due to the fact that the less dense pyrope-rich almandine garnet is more frequent in the coarse grain-size fraction, hydraulic sorting according to their density can be excluded and it is more likely that this is an effect of grain-size distribution in the source rocks.

The short axes of the garnets lie within the expected interval of 63−125 µm, except of a few grains. The long axes show a wider distribution in their sizes (>80−260 µm) (Fig. 4; Table 2). Most of the long axes (38−86 %) are longer in size than the sieved grain-size fraction (Fig. 4; Table 2). This means that a wet-sieved sample is only separated by the short axes of the minerals. Therefore, it is possible that grains with a short axis of 120 µm and a long axis of 480 µm, for instance, occur in the 63−125 µm grain-size fraction although their average grain size may be around 300 µm. The highest concentration of garnet grains occurs in the 125−500 µm grain-size fraction (Fig. 3b). This also points, in contrast to e.g. apatite, to a generally coarser garnet grain size in the source rocks.

6. Conclusions

The heavy mineral assemblages reflect the geological situation in the area of Almklovdalen. The dominant heavy mineral is olivine. From upstream to downstream the content of olivine strongly increases, whereas the content of all other heavy minerals found in the samples strongly decreases. This is because in the upstream part of the sampled river the diversity of potential source rocks is higher than in the downstream part of the river where the proportion of dunite and chlorite peridotite is much higher. Garnets with high MgO content are more frequent in the coarse grain-size fractions, which likely result from the inheritance of grain size from source rock to sediment. However, only very few garnets of the 250−1000 μm grain-size fractions show full overlap with the garnets from the garnet peridotite sample. In contrast, garnets with high MnO content are more frequent in the fine grain-size fractions. Therefore, analysing a wide grain-size window is of paramount importance, as also discussed in other studies (e.g., Garzanti et al., 2009; Krippner et al., 2015), because we can miss information contained in other grain-size fractions.

Acknowledgments

The PhD scholarship of AK is financed by CASP. Fieldwork and analytical work was financed by the German Research Foundation (DFG grant EY 23/20-1). We thank Andreas Kronz for his help with EMP analyses. Constructive reviews were provided by Sergio Andò and Alberto Resentini.

Appendix A. Supplementary data

Supplementary data associated with this article can be found, in the online version, at xxx.

References

Aitchison, J., 1986. The Statistical Analysis of Compositional Data, Monographs on Statistics and Applied Probability. Chapman & Hall Ltd., London, 416 pp.

Andersen, T.B., Jamtveit, B., Dewey, J.F., Swensson, E., 1991. Subduction and eduction of continental crust: major mechanism during continent-continent collision and orogenic collapse, a model based on the south Norwegian Caledonides. Terra Nova 3, 303–310.

370 Andò, S., 2007. Heavy minerals: provenance, hydraulic sorting, weathering. Unpublished PhD Thesis,
371 University of Milano-Bicocca, 210 pp.
372 Andò, S., Garzanti, E., Padoan, M., Limonta, M., 2012. Corrosion of heavy minerals during
373 weathering and diagenesis: A catalog for optical analysis. Sedimentary Geology 208, 165–178.
374 Andò, S., Morton, A.C., Garzanti, E., 2013. Metamorphic grade of source rocks revealed by chemical
375 fingerprints of detrital amphibole and garnet. In: Scott, R.A., Smyth, H.R., Morton, A.C.,
376 Richardson, N. (Eds.), Sediment Provenance Studies in Hydrocarbon Exploration and
377 Production. Geological Society, London, Special Publication 386, pp. 351–371.
378 Beyer, E.E., Brueckner, H.K., Griffin, W.L., O'Reilly, S.Y., Graham, S., 2004. Archean mantle
379 fragments in Proterozoic crust, Western Gneiss Region, Norway. Geology 32, 609–612.
380 Beyer, E.E., Griffin, W.L., O'Reilly, S.Y., 2006. Transformation of Archean lithospheric mantle by
381 refertilization: Evidence from exposed peridotites in the Western Gneiss Region, Norway.
382 Geology 32, 609–612.
383 Beyer, E.E., Brueckner, H.K., Griffin, W.L., O'Reilly, S.Y., 2012. Laurentian Provenance of Archean
384 Mantle Fragments in the Proterozoic Baltic Crust of the Norwegian Caledonides. Journal of
385 Petrology 53, 1357–1383.
386 Brueckner, H.K., Carswell, D.A., Griffin, W.L., 2002. Paleozoic diamonds within a Precambrian
387 peridotite lens in UHP gneisses of the Norwegian Caledonides. Earth and Planetary Science
388 Letters 203, 805−816.
389 Brueckner, H.K., Carswell, D.A., Griffin, W.L., Medaris, L.G., van Roermund, H.L.M., Cuthbert, S.J.,
390 2010. The mantle and crustal evolution of two garnet peridotite suites from the Western Gneiss
391 Region, Norwegian Caledonides: an isotopic investigation. Lithos 117, 1−19.
392 Bryhni, I., Andréasson, P.G, 1985. Metamorphism in the Scandinavian Caledonides. In: Gee, D.G.,
393 Sturt, B.A. (Eds.), The Caledonide Orogen – Scandinavia and Related Areas. Wiley, Chichester,
394 763−781.
395 Carswell, D.A., 1986. The metamorphic evolution of Mg–Cr type Norwegian garnet peridotites.
396 Lithos 19, 279–297.

397 Carswell, D.A., Cuthbert, S.J., 2003. Review of the mineralogical and microstructural evolution of
398 ultra-high pressure eclogites in the Western Gneiss Region of Norway. In: Carswell, D.A.,
399 Cuthbert, S.J., Krabbendam, M., Medaris, L.G., Brueckner, H.K. (Eds.), Guidebook to the Field
400 Exkursions in the Nordfjord - Stadtlandet - Almklovdalen Area. NGU Report, pp. 3−47.
401 Comas-Cufí, M., Thió-Henestrosa, S., 2011. CoDaPack 2.0: a stand-alone, multi-platform
402 compositional software. In: Egozcue, J.J., Tolosana-Delgado, R., Ortego, M.I. (Eds.),
403 CoDaWork'11: 4th International Workshop on Compositional Data Analysis. Sant Feliu de
404 Guíxols (http://congress.cimne.com/codawork11/Admin/Files/FilePaper/p28.pdf).
405 Cordellier, F.M., Boudier, F., Boullier, A.M., 1981. Structural study of the Almklovdalen peridotite
406 massif (southern Norway). Tectonophysics 77, 257−281.
407 Cuthbert, S.J., Carswell, D.A., Krogh-Ravna, E.J., Wain, A. 2000. Eclogites and eclogites of the
408 Western Gneiss Region, Norwegian Caledonides. Lithos 52, 165−195.
409 Deer, W.A., Howie, R.A., Zussman, J., 1992. An introduction to rock-forming minerals. Longman
410 Group Ltd, Harlow, UK, 712 pp.
411 Eskola, P., 1921. On the eclogites of Norway. Skrifter udgivne af Videnskabs-Selskapet i Christiana,
412 Matematisk-Naturvidenskapelig Klasse 8, 1–118.
413 Garzanti, E., Andò, S., Vezzoli, G., 2008. Settling-equivalence of detrital minerals and grain-size
414 dependence of sediment composition. Earth and Planetary Science Letters 273, 138–151.
415 Garzanti, E., Andò, S., Vezzoli, G., 2009. Grain-size dependence of sediment composition and
416 environmental bias in provenance studies. Earth and Planetary Science Letters, 277, 422–432.
417 Garzanti, E., Resentini, A., Vezzoli, G., 2010. Detrital fingerprints of fossil continental-subduction
418 zones (Axial Belt Provenance, European Alps). Journal of Geology 118, 341–362.
419 Garzanti, E., Limonta, M., Resentini, A., Bandopadhyay, P.C., Najman, Y., Andò, S., Vezzoli, G.,
420 2013. Sediment recycling at convergent plate margins (Indo-Burman Ranges and Andaman–
421 Nicobar Ridge. Earth-Science Reviews 123, 113–132.
422 Gebauer, D., Lappin, M.A., Grunenfelder, M., Wyttenbach, A. 1985. The age and origin of some
423 Norwegian eclogites: a U-Pb zircon and REE study. Chemical Geology 52, 22−47.

Griffin, W.L., Brueckner, H.K., 1980. Caledonian Sm-Nd ages and a crustal origin of Norwegian eclogites. Nature 285, 319−21.

Griffin, W.L., Qvale, H., 1985. Superferrian eclogites and the crustal origin of garnet peridotites. Almklovdalen, Norway. In: Gee, D.G., Sturt, B.A. (Eds.), The Caledonide Orogen – Scandinavia and Related Areas. Wiley, Chichester, pp. 763−781.

Griffin, W.L., Austrheim, H., Brastad, K., Bryhni, I., Krill, A.G., Krogh, E.J., Mørk, M.B.E., Qvale, H., Torudbakken, B., 1985. High-pressure metamorphism in the Scandinavien Caledonides. In: Gee, D.G., Sturt, B.A. (Eds.), The Caledonide Orogen – Scandinavia and Related Areas. Wiley, Chichester, pp. 783−801.

Grütter, H.S., Gurney, J.J., Menzies, A.H., Winter, F., 2004. An updated classification scheme for mantle-derived garnets, for use by diamond explorers. Lithos 77, 841–857.

Gurney, J.J., 1984. A correlation between garnets and diamonds. In: Glover, J.E., Harris, P.G. (Eds.), Kimberlite occurrence and origins: a Basis for Conceptual Models in Exploration. Geology Department and University Extension, University of Western Australia, Publication 8, 143–166.

Krogh, E.J., 1977. Evidence for a Precambrian continent-continent collision in western Norway. Nature 267, 17−19.

Krabbendam, M., Wain, A., 1997. Late-Caledonian structures, differential regression and structural position of (ultra)high-pressure rocks in the Nordfjord-Stradlandet area, Western Gneiss Region. Norges Geologiske Undersøkelse 432, 127−139.

Krabbendam, M., Wain, A., Andersen, T.B., 2000. Pre-Caledonian granulite and gabbro enclaves in the Western Gneiss Region, Norway: indications of incomplete transition at high pressure. Geological Magazine 137, 235−255.

Krippner, A., Meinhold, G., Morton, A.C., von Eynatten, H., 2014. Evaluation of garnet discrimination diagrams using geochemical data derived from various host rocks. Sedimentary Geology 306, 36–52.

Krippner, A., Meinhold, G., Morton, A.C., Russell, E., von Eynatten, H., 2015. Grain-size dependence of garnet composition revealed by provenance signatures of modern stream sediments from the western Hohe Tauern (Austria). Sedimentary Geology, 321, 25–38.

452 Mange, M.A., Maurer, H.F.W., 1992. Heavy Minerals in color, Chapman and Hall, London, 147 pp.
453 Mange, M.A., Morton, A.C., 2007. Geochemistry of heavy minerals. In: Mange, M.A., Wright, D.T.
454 (Eds.), Heavy Minerals in Use. Developments in Sedimentology 58, Elsevier, Amsterdam, pp.
455 345–391.
456 Mange, M.A, Wright, D.T., 2007. Heavy Minerals in Use. Developments in Sedimentology 58,
457 Elsevier, Amsterdam, 1329 pp.
458 Medaris, L.G., 1984. A geothermobarometric investigation of garnet peridotites in the Western Gneiss
459 Region of Norway. Contributions to Mineralogy and Petrology 87, 72–86.
460 Medaris, L.G., Carswell, D.A., 1990. The petrogenesis of Mg–Cr garnet peridotites in European
461 metamorphic belts. In: Carswell, D.A. (Ed.), Eclogite Facies Rocks. New York, Chapman and
462 Hall, pp. 260–290.
463 Medaris, L.G., Brueckner, H.K., 2003. Excursion to the Almklovdalen Peridotite. In: Carswell, D.A.,
464 Cuthbert, S.J., Krabbendam, M., Medaris, L.G., Brueckner, H.K. (Eds.), Guidebook to the Field
465 Exkursions in the Nordfjord - Stadtlandet - Almklovdalen Area, NGU Report, pp. 109–133.
466 Meinhold, G., Reischmann, T., Kostopoulos, D., Frei, D., Larionov, A.N., 2010. Mineral chemical and
467 geochronological constraints on the age and provenance of the eastern Circum-Rhodope Belt
468 low-grade metasedimentary rocks, NE Greece. Sedimentary Geology 229, 207–223.
469 Mørk, M.B.E., Mearns, E.W., 1985. Sm-Nd isotopic systematics of a gabbro-eclogite transition.
470 Lithos 19, 255–267.
471 Morton, A.C., 1985. A new approach to provenance studies: electron microprobe analysis of detrital
472 garnets from Middle Jurassic sandstones of the northern North Sea. Sedimentology 32, 553–566.
473 Morton, A.C., 2012. Value of heavy minerals in sediments and sedimentary rocks for provenance,
474 transport history and stratigraphic correlation. In: Sylvester, P. (Ed.), Quantitative Mineralogy
475 and Microanalysis of Sediments and Sedimentary Rocks. Mineralogical Association of Canada
476 Short Course Series 42, pp. 133–165.
477 Morton, A.C., Hallsworth, C.R., 1999. Processes controlling the composition of heavy mineral
478 assemblages in sandstones. Sedimentary Geology 124, 3–29.

Morton, A.C., Whitham, A.G., Fanning, C.M., 2005. Provenance of Late Cretaceous to Paleocene submarine fan sandstones in the Norwegian Sea: integration of heavy mineral, mineral chemical and zircon age data. Sedimentary Geology 182, 3–28.

Morton, A.C., Meinhold, G., Howard, J.P., Phillips, R.J., Strogen, D., Abutarruma, Y., Elgadry, M., Thusu, B., Whitham, A.G., 2011. A heavy mineral study of sandstones from the eastern margin of the Murzuq Basin, Libya: constraints on provenance and stratigraphic correlation. Journal of African Earth Sciences 61, 308–330.

Nowicki, T., Dyck, D., Carlson, J., Helmstaedt, H., 2003. The geology of kimberlite pipes of the Ekati property, Northwest Territories, Canada. Lithos 76, 1–27.

Osland, R., 1997. Modelling of variations in Norwegian olivine deposits, causes of variation and estimation of key quality factors. Doktor Ingeniør thesis, Norwegian University of Science and Technology, 189 pp.

Pettijohn, F.J., 1941. Persistence of heavy minerals and geological age. Journal of Geology 49, 610–625.

Resentini, A., Malusà, M.G., Garzanti, E., 2013. MinSORTING: An Excel® worksheet for modelling mineral grain-size distribution in sediments, with application to detrital geochronology and provenance studies. Computers & Geosciences 59, 90–97.

Rittenhouse, G., 1943. Transportation and deposition of heavy minerals. Geological Society America Bulletin 54, 1725–1780.

Roberts, D.C., Gee, D.G., 1985. An introduction to the structure of the Scandinavian Caledonides. In: Gee, D.G., Sturt, B.A. (Eds.), The Caledonide Orogen – Scandinavia and Related Areas. Wiley, Chichester, 55–68.

Root, D.B., Hacker, B.R., Gans, P.B., Duccea, M.N., Eide, E.A., Mosenfelder, L., 2005. Discrete ultrahigh-pressure domains in the Western Gneiss Region, Norway: Implications for formation and exhumation. Journal of Metamorphic Geology 23, 45–61.

Rubey, W.W., 1933. The size-distribution of heavy minerals within a water-laid sandstone. Journal of Sedimentary Petrology 3, 3–29.

506 Schuiling, R.D., de Meijer, R.J., Riezebos, H.J., Scholten, M.J., 1985. Grain-size distribution of
507 different minerals in a sediment as a function of their specific density. Geologie en Mijnbouw 64,
508 199–203.
509 Thió-Henestrosa, S., Martín-Fernández, J.A., 2005. Dealing with compositional data: the freeware
510 CoDaPack. Mathematical Geology 37, 773–793.
511 Tucker, R.D., Krogh, T.E., Råheim, A., 1990. Proterozoic evolution and age-province boundaries in
512 the central part of the Western Gneiss Region, Norway; results of U-Pb dating of accessory
513 minerals from Trondheimsfjord to Geieranger. In: Gower, C.F., Rivers, T., Ryan, B. (Eds.), Mid-
514 Proterozoic Laurentia-Baltica. Geological Association of Canada, Special Paper 38, pp. 149–173.
515 van Andel, T.H., 1950. Provenance, transport and deposition of Rhine sediments: a heavy mineral
516 study on river sands from the drainage area of the Rhine. Dissertation, Rijksuniversiteit te
517 Groningen, Veenman & Zonen, Wageningen, 129 pp.
518 Velbel, M.A., 2007. Surface textures and dissolution processes of heavy minerals in the sedimentary
519 cycle: examples from pyroxenes and amphiboles. In: Mange, M., Wright, D.K. (Eds.), Heavy
520 Minerals In Use. Developments in Sedimentology 58, Elsevier, Amsterdam, pp. 112–150.
521 Velbel, M.A., 1984. Natural weathering mechanisms of almandine garnet. Geology 12, 631–634.
522 Velbel, M.A., 1999. Bond strength and the relative weathering rates of simple orthosilicates. American
523 Journal of Science 299, 679–696.
524 von Eynatten, H., Barceló-Vidal, C., Pawlowsky-Glahn, V., 2003. Composition and discrimination of
525 sandstones: A statistical evaluation of different analytical methods. Journal of Sedimentary
526 Research 73, 47–57.
527 von Eynatten, H., Dunkl, I., 2012. Assessing the sediment factory: the role of single grain analysis.
528 Earth-Science Reviews 115, 97–120.
529 Whitham, A.G., Morton, A.C., Fanning, C.M., 2004. Insights into Cretaceous–Palaeogene sediment
530 transport paths and basin evolution in the North Atlantic from a heavy mineral study of
531 sandstones from southern East Greenland. Petroleum Geoscience 10, 61–72.
532 Wright, W.I., 1938. The composition and occurrence of garnets. American Mineralogist 23, 436–449
533

Tables

Table 1. Geographic coordinates (WGS 84) of all samples (river sediments and bedrocks) from the Almklovdalen area.

Table 2. Operating conditions of the electron microprobe for garnet analyses. *Count time* on the peak (in s), *Bckg time* counting time on background position (in s), *DL* detection limit (in ppm).

Table 3. Mineralogy of the bedrock samples.

Figure captions

Fig.1. Map of the outer Nordfjord and Stradlandet area of the Western Gneiss Region showing the distribution of ultramafic bodies. Dashed lines mark the limits of the HP and UHP zones and the extent of the mixed HP/UHP zone (adapted from Carswell and Cuthbert, 2003). The inset shows the location of the study area in the SW part of the Caledonides in Norway.

Fig. 2. Geological map of the Almklovdalen area (adapted from Medaris and Brueckner, 2003) showing sample locations. The eclogite occurrences have sizes up to several meters and are enclosed within both the gneisses and peridotites.

Fig. 3. a) Transparent heavy mineral suite of the 63–125 µm grain-size fraction of the analysed samples. **b)** Heavy mineral distribution of all grain-size fractions of samples AK-N19-3. Epidote-group: epidote, zoisite; ultrastable minerals: zircon, rutile, tourmaline; others: titanite, other amphibole (excluding green calcic amphibole).

Fig. 4. Grain-size distribution of the short and the long axes of garnets from stream sediments of the 63−125 µm grain-size fraction (upper part) and of the eclogite samples AK-N21 and AK-EA (lower part).

563

564 **Fig. 5.** Compositional biplot of garnets based on major elements Al_2O_3, SiO_2, CaO, FeO, MnO, and
565 MgO. Axes are first and second principal components (PC). **a)** Compositional biplot of garnet grains
566 from the bedrocks. Almost 73% of the variability is explained by the first PC and 13% by the second
567 PC. **b)** Compositional biplot of detrital garnet grains from the bedrocks and from all stream sediments
568 of the 63−125 μm grain-size fraction. Almost 51% of the variability is explained by the first PC and
569 20% by the second PC. **c)** Compositional biplot from sample AK-N19-3 of the 63−125 μm, 125−250
570 μm, 250−500 μm, and 500−1000 μm grain-size fractions. Almost 49% of the variability is explained
571 by the first PC and 20% by the second PC.

572

573 **Fig. 6.** Composition of garnets in the ternary classification diagram of Mange and Morton (2007) with
574 almandine+spessartine, grossular and pyrope as poles. **a)** Composition of garnets from the bedrock
575 samples. **b)** Composition of detrital garnets of the 63−125 μm grain-size fraction and from the bedrock
576 samples. **c)** Composition of detrital garnets of the 125−250 μm, 250−500 μm, and 500−1000 μm
577 grain-size fraction and from the bedrock samples. A – mainly from high-grade granulite-facies
578 metasedimentary rocks or charnockites and intermediate felsic igneous rocks, B – amphibolite-facies
579 metasedimentary rocks, Bi – intermediate to felsic igneous rocks, Ci – mainly from high-grade mafic
580 rocks, Cii – ultramafics with high Mg (pyroxenites and peridotites), D – metasomatic rocks, very low-
581 grade metamafic rocks and ultrahigh–temperature metamorphosed calc-silicate granulites.

582

583 **Fig. 7.** Binary diagram showing CaO/MnO vs. MgO/MnO garnet values of all grain-size fractions of
584 sample AK-N19-3.

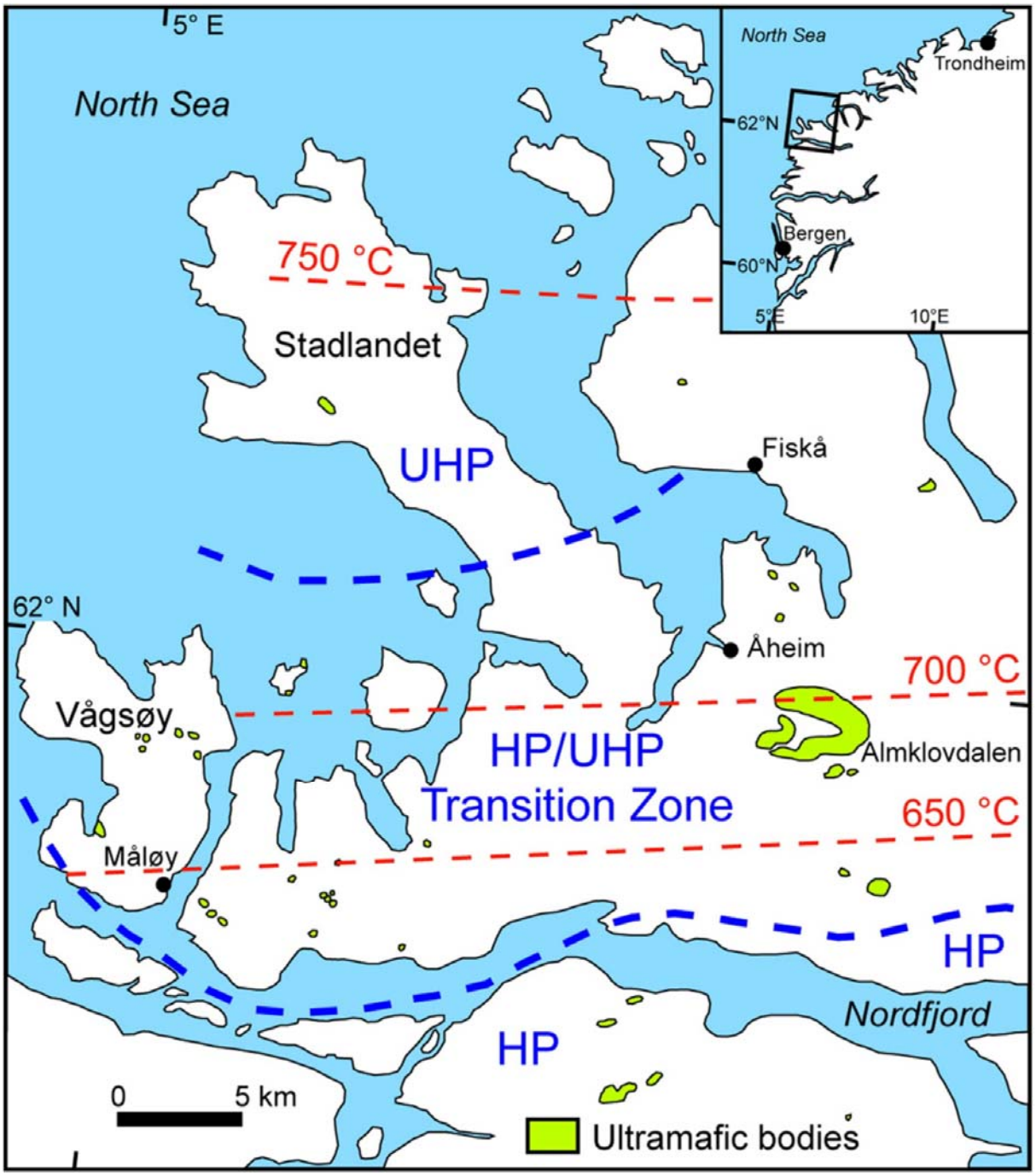
5° E
North Sea
750 °C
Stadlandet
UHP
Fiská
62° N
Åheim
700 °C
Vågsøy
HP/UHP
Transition Zone
Almklovdalen
650 °C
Måløy
HP
Nordfjord
HP
0
5 km
Ultramafic bodies
North Sea
Trondheim
62°N
Bergen
60°N
5°E
10°E

Fig. 1

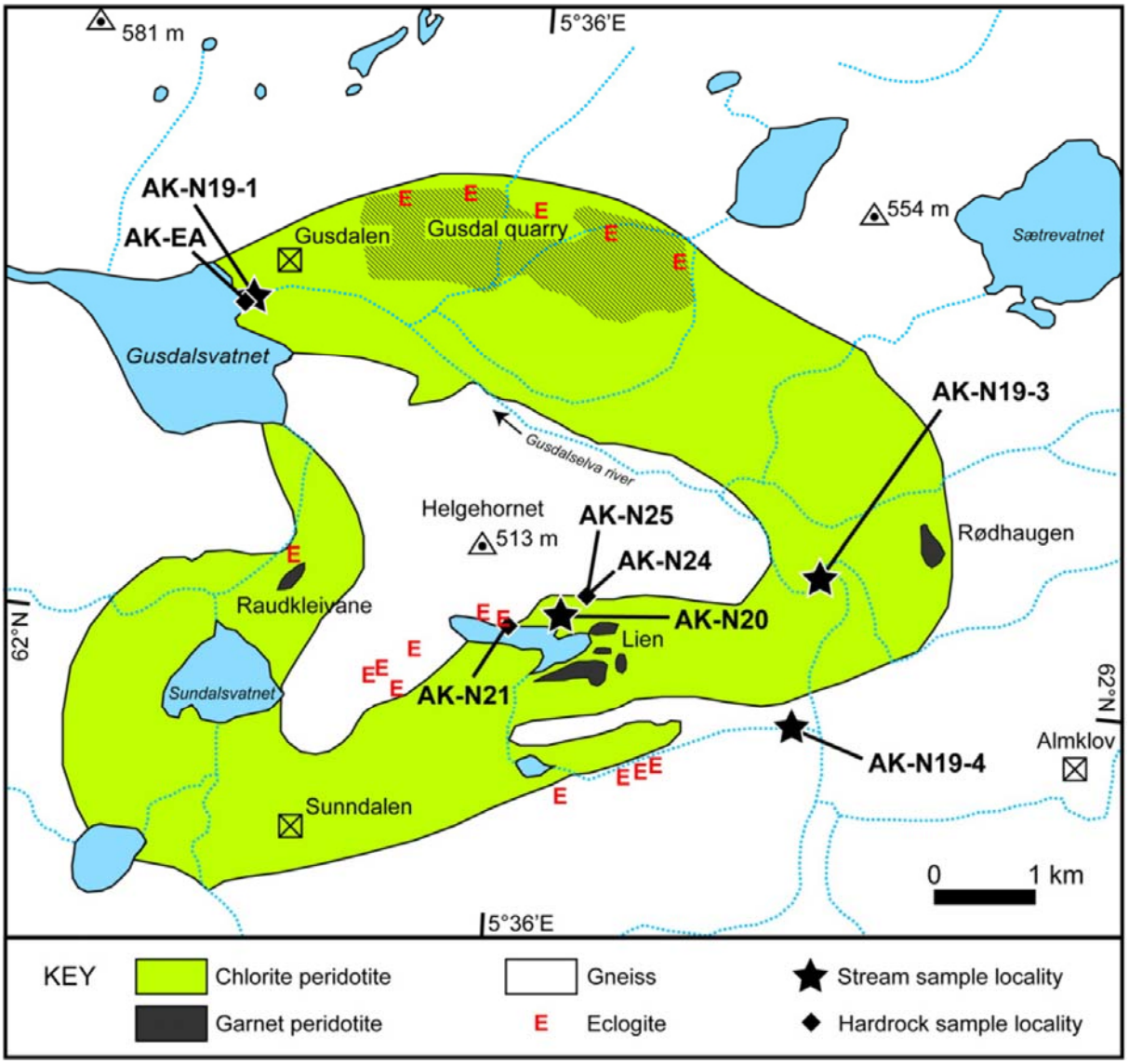
581 m
5°36'E
AK-N19-1
AK-EA
Gusdalen
Gusdal quarry
554 m
Sætrevatnet
Gusdalsvatnet
AK-N19-3
Gusdalselva river
Helgehornet
513 m
AK-N25
AK-N24
Rødhaugen
Raudkleivane
AK-N20
Lien
62°N
Sundalsvatnet
AK-N21
62°N
AK-N19-4
Almklov
Sunndalen
0
1 km
5°36'E
KEY
Chlorite peridotite
Gneiss
Stream sample locality
Garnet peridotite
E
Eclogite
Hardrock sample locality

Fig. 2

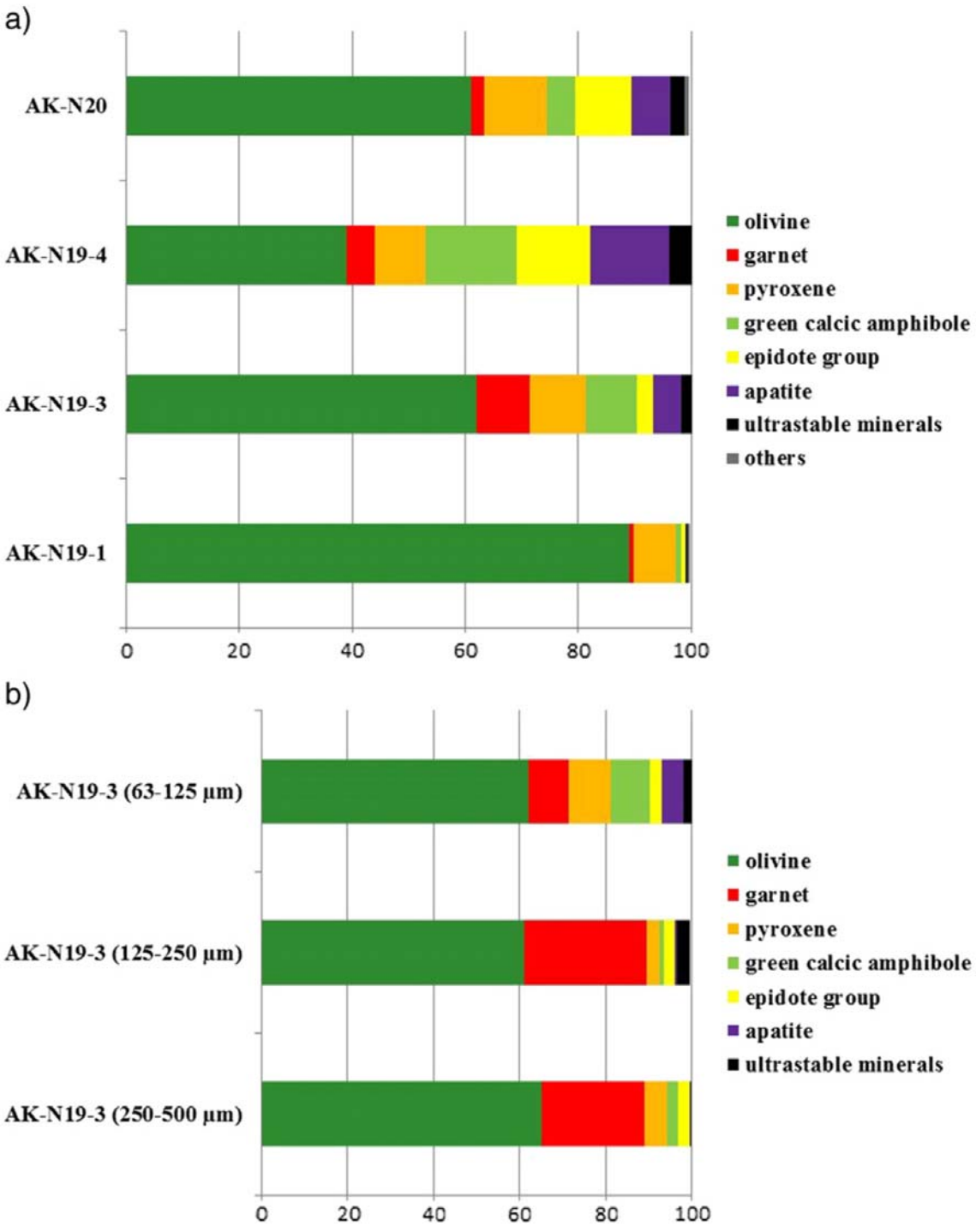
a)
AK-N20
AK-N19-4
AK-N19-3
AK-N19-1
0
20
40
60
80
100
olivine
garnet
pyroxene
green calcic amphibole
epidote group
apatite
ultrastable minerals
others
b)
AK-N19-3 (63-125 µm)
AK-N19-3 (125-250 µm)
AK-N19-3 (250-500 µm)
0
20
40
60
80
100
olivine
garnet
pyroxene
green calcic amphibole
epidote group
apatite
ultrastable minerals

Fig. 3

Stream Sediments

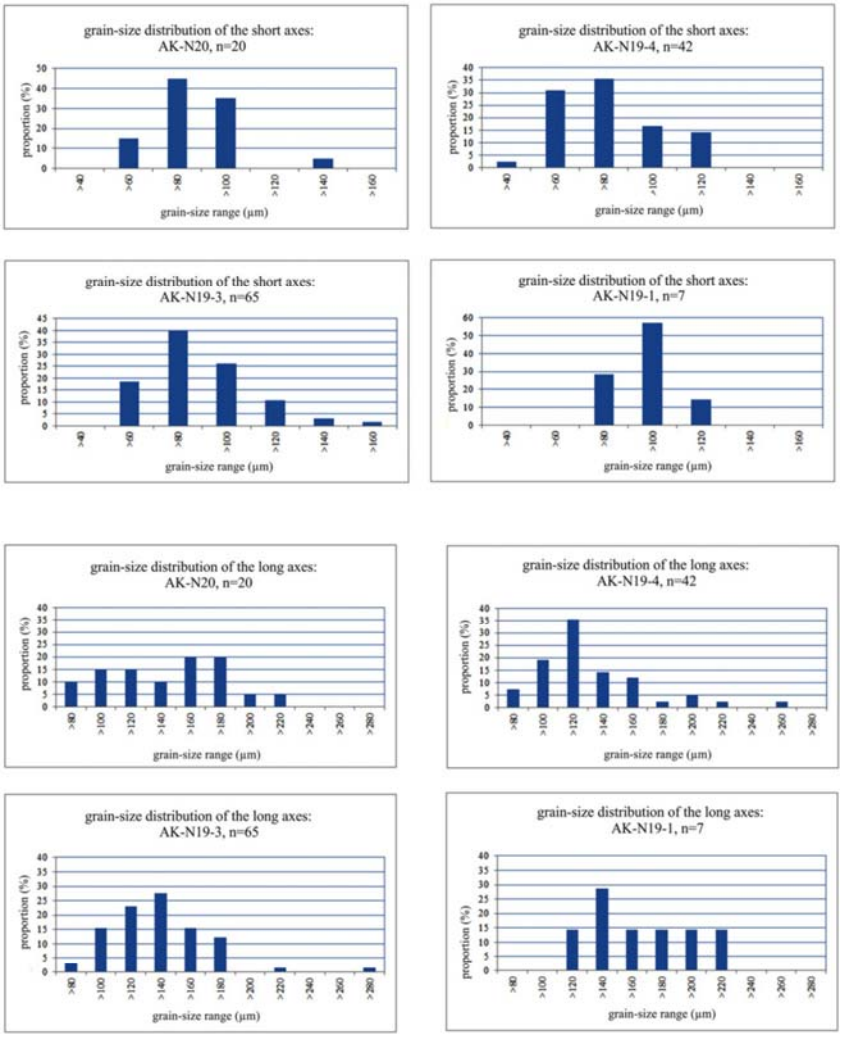

Bedrocks

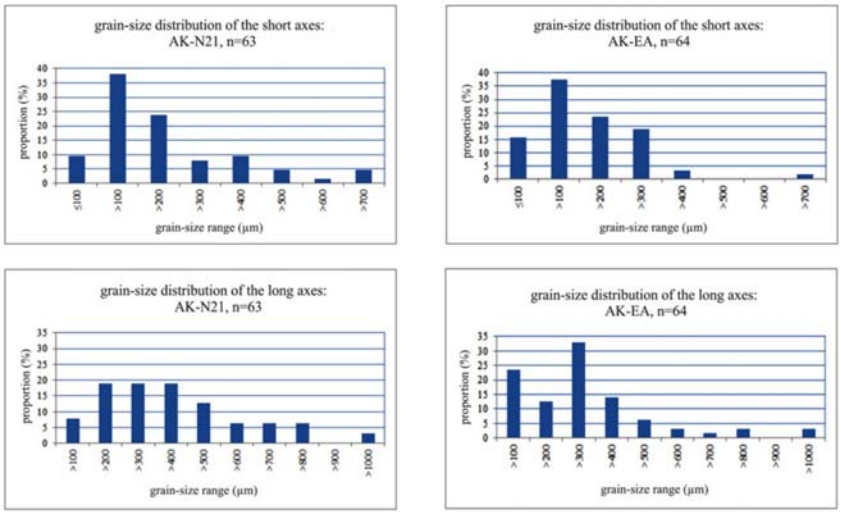

Fig. 4

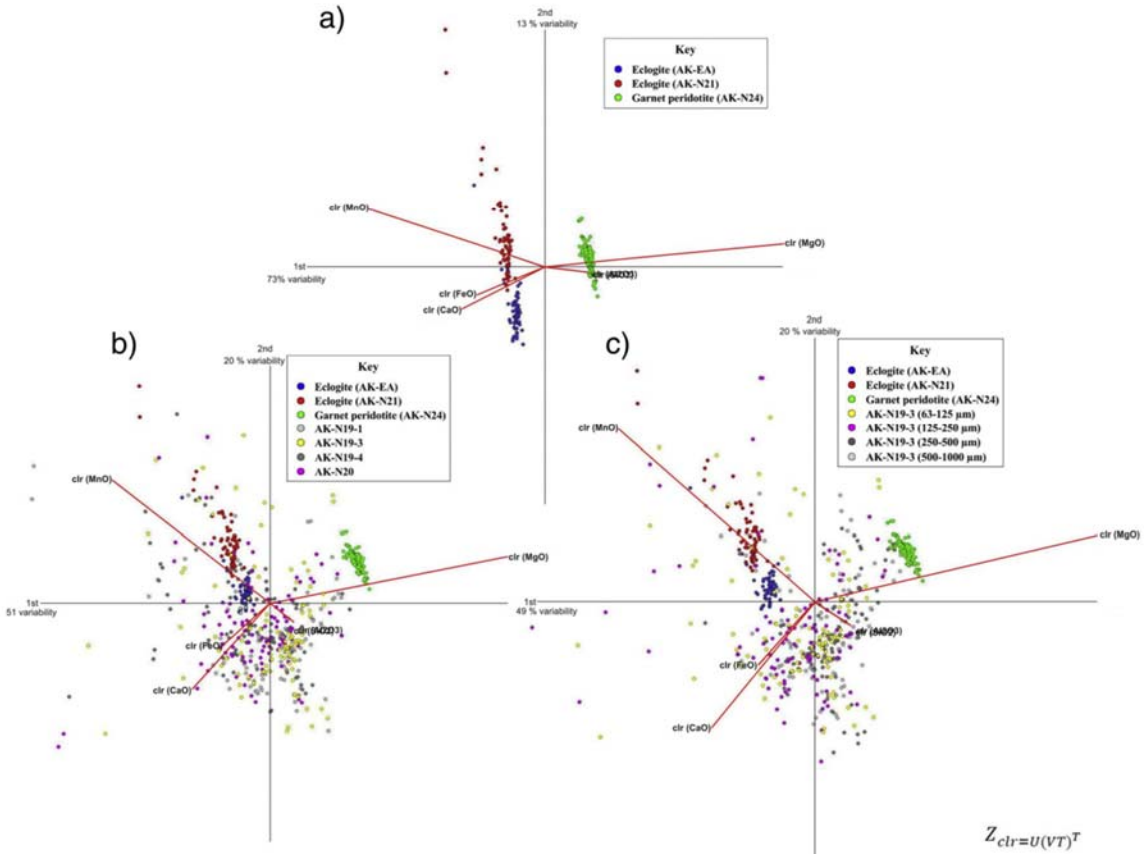
a)
2nd
13 % variability
Key
Eclogite (AK-EA)
Eclogite (AK-N21)
Garnet peridotite (AK-N24)
clr (MnO)
clr (MgO)
1st
73% variability
clr (FeO)
clr (CaO)
b)
2nd
20 % variability
Key
Eclogite (AK-EA)
Eclogite (AK-N21)
Garnet peridotite (AK-N24)
AK-N19-1
AK-N19-3
AK-N19-4
AK-N20
clr (MnO)
clr (MgO)
1st
51 variability
clr (FeO)
clr (CaO)
c)
2nd
20 % variability
Key
Eclogite (AK-EA)
Eclogite (AK-N21)
Garnet peridotite (AK-N24)
AK-N19-3 (63-125 µm)
AK-N19-3 (125-250 µm)
AK-N19-3 (250-500 µm)
AK-N19-3 (500-1000 µm)
clr (MnO)
clr (MgO)
1st
49 % variability
clr (FeO)
clr (CaO)
$Z_{clr=U(VT)^T}$

Fig. 5

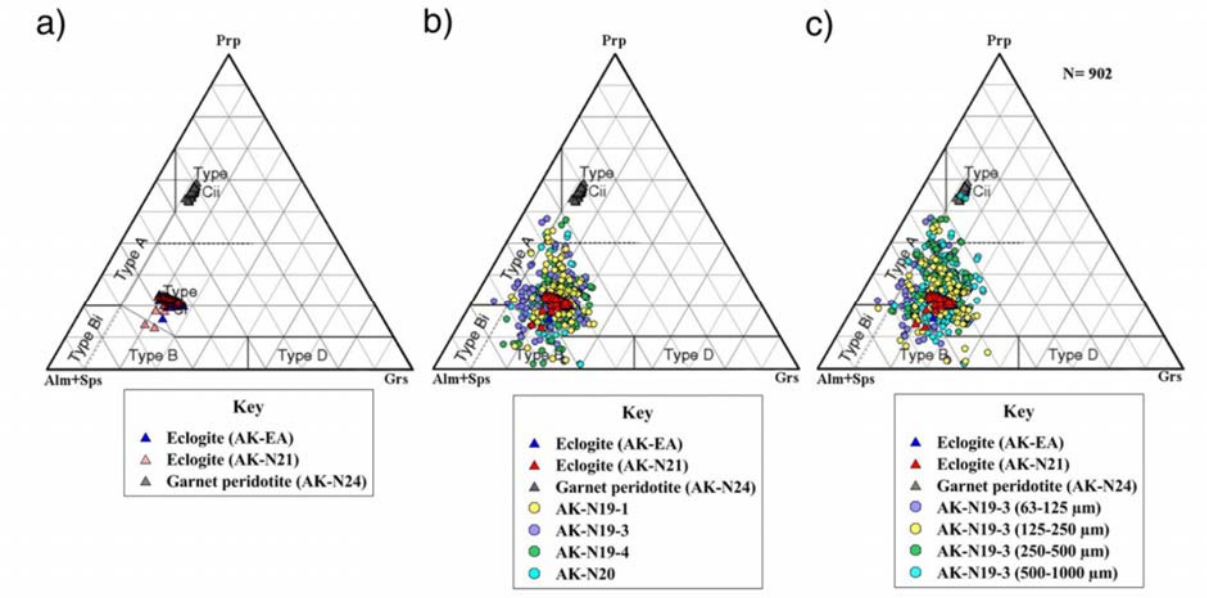
a)
Prp
Type Cii
Type A
Type Bi
Type B
Type D
Alm+Sps
Grs
Key
Eclogite (AK-EA)
Eclogite (AK-N21)
Garnet peridotite (AK-N24)
b)
Prp
Type Cii
Type A
Type Bi
Type B
Type D
Alm+Sps
Grs
Key
Eclogite (AK-EA)
Eclogite (AK-N21)
Garnet peridotite (AK-N24)
AK-N19-1
AK-N19-3
AK-N19-4
AK-N20
c)
Prp
N= 902
Type Cii
Type A
Type Bi
Type B
Type D
Alm+Sps
Grs
Key
Eclogite (AK-EA)
Eclogite (AK-N21)
Garnet peridotite (AK-N24)
AK-N19-3 (63-125 µm)
AK-N19-3 (125-250 µm)
AK-N19-3 (250-500 µm)
AK-N19-3 (500-1000 µm)

Fig. 6

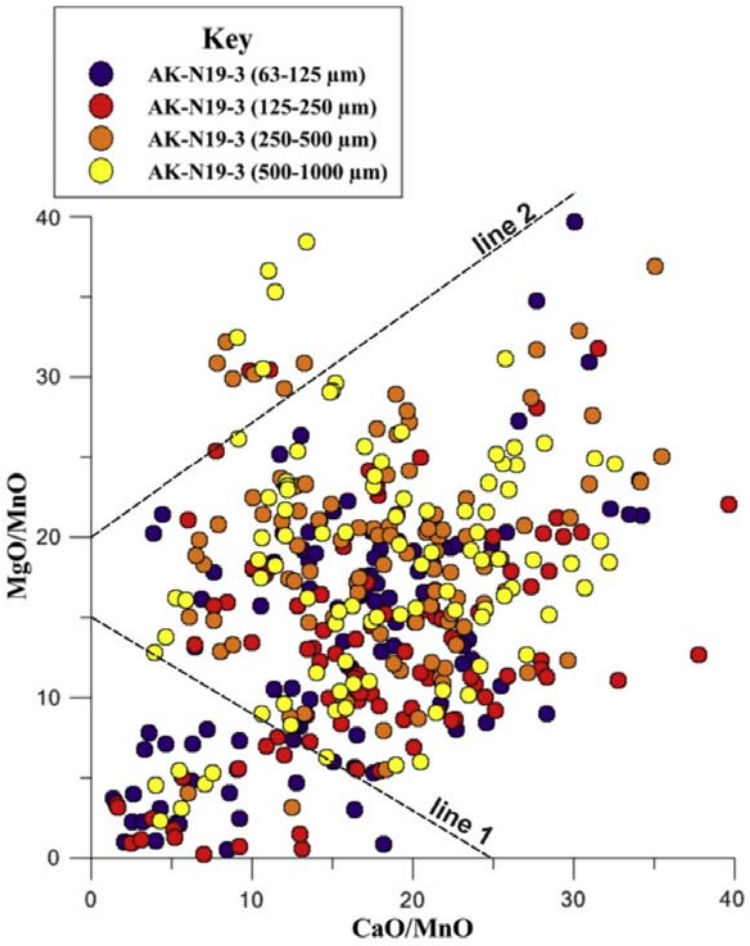
Key
AK-N19-3 (63-125 µm)
AK-N19-3 (125-250 µm)
AK-N19-3 (250-500 µm)
AK-N19-3 (500-1000 µm)
line 2
line 1
MgO/MnO
CaO/MnO
0
10
20
30
40

Fig. 7

Table 1

Sample	Bedrock/sediment	GPS: N°	GPS: E°
AK-N20	Sediment	62°00.202'	5°36.268'
AK-N19-4	Sediment	62°00.001'	5°37.573'
AK-N19-3	Sediment	62°00.315'	5°37.690'
AK-N19-1	Sediment	62°01.010'	5°34.417'
AK-N21	Eclogite	62°00.153'	5°35.998'
AK-EA	Eclogite	62°01.010'	5°34.417'
AK-N24	Garnet peridotite	62°00.278'	5°36.448'
AK-N25	Gneiss	62°00.278'	5°36.448'

Table 2

Spectrometer	1 TAP	1 TAP	2 TAP	3 PETJ	4 PETJ	4 PETJ	5 LIFH	5 LIFH
Element (line)	Si (Kα)	Al (Kα)	Mg (Kα)	Ca (Kα)	Ti (Kα)	Cr (Kα)	Mn (Kα)	Fe (Kα)
Count time	15	15	15	15	30	30	30	15
Bckg time	5	5	5	5	15	15	15	5
Standard	Garnet natural	Garnet natural	MgO synthetic	$CaSiO_3$ natural	TiO_2 synthetic	Cr_2O_3 synthetic	Rhodonite natural	Fe_2O_3 synthetic
DL	160	138	104	138	113	135	117	216

Table 3

Mineral/sample	AK-N21 (eclogite)	AK-EA (eclogite)	AK-N24 (grt-peridotite)	AK-N25 (gneiss)
Quartz	++	++	○	+++
K-feldspar	−	−	−	+
Plagioclase	○	○	−	+
Micas	○	○	++	○
Pyroxene	++	++	○	−
Amphibole	+	+	++	○
Olivine	+	+	+++	−
Garnet	+	+	++	−
Rutile	t	t	−	+
Zircon	+	+	−	○
Titanite	−	−	−	+
Apatite	−	−	−	+

+++, very high content; ++, high content; ○, low content; *t*, traces; −, not present.